GeoDa Center
FOR GEOSPATIAL ANALYSIS
AND COMPUTATION

ARIZONA STATE UNIVERSITY

Working Paper 2011-05

Improving the Multi-Dimensional Comparison of Simulation Results: A Spatial Visualization Approach

Daniel Arribas-Bel, Julia Koschinsky and Pedro Amaral

Improving the Multi-Dimensional Comparison of Simulation Results: A Spatial Visualization Approach

Daniel Arribas-Bel* Julia Koschinsky† Pedro V. Amaral‡

August 8, 2011

Abstract

Results from simulation experiments are important in applied spatial econometrics to, for instance, assess the performance of spatial estimators and tests for finite samples. However, the traditional tabular and graphical formats for displaying simulation results in the literature have several disadvantages. These include loss of results, lack of intuitive synthesis, and difficulty in comparing results across multiple dimensions. We propose to address these challenges through a spatial visualization approach. This approach visualizes model precision and bias as well as the size and power of tests in map format. The advantage of this spatial approach is that these maps can display all results succinctly, enable an intuitive interpretation, and compare results efficiently across multiple dimensions of a simulation experiment. Due to the respective strengths of tables, graphs and maps, we propose this spatial approach as a supplement to traditional tabular and graphical display formats.

Keywords spatial visualization; Monte Carlo simulation experiments; spatial econometrics.

JEL Y1, C5

1 Introduction

Insight about the relative performance of different spatial econometric tests, estimators, weights and specification strategies in finite samples is frequently

*GeoDa Center for Geospatial Analysis and Computation, School of Geographical Sciences and Urban Planning, Arizona State University, Tempe, USA. darribas@asu.edu

†GeoDa Center for Geospatial Analysis and Computation, School of Geographical Sciences and Urban Planning, Arizona State University, Tempe, USA. julia.koschinsky@asu.edu

‡GeoDa Center for Geospatial Analysis and Computation, School of Geographical Sciences and Urban Planning, Arizona State University, Tempe, USA; and Land Economy Department, University of Cambridge. pedro.amaral@asu.edu@asu.edu

obtained from Monte Carlo simulation experiments (see Anselin and Rey, 1991 and Florax and de Graaff, 2004 for summaries). Such knowledge is relevant to guide choices in applied spatial research where theoretical spatial econometric assumptions of asymptotics might not hold. Results from simulation experiments are inherently multi-dimensional as they reflect dimensions such as different spatial tests or estimators, spatial parameters, sample sizes, data generating processes, and weights matrices. However, standard existing formats of reporting this multi-dimensionality are associated with several key challenges: 1) Many results are not displayed because the output far exceeds an article's allowable space limit (e.g. Baltagi et al, 2003 p.132 footnote 2 and Anselin and Moreno, 2003, p. 605, footnote 19); 2) the generally overwhelming volume of results reported in traditional tabular format hinders an immediate intuitive interpretation; and 3) traditional tabular and graphical reporting formats make it difficult to efficiently compare results across tables and graphs, respectively.

The purpose of this article is to propose a spatial visualization approach to mapping simulation results that address these three challenges. Although spatial econometric simulation results pertain to spatial methods, spatial approaches have rarely been used to display these results. What a spatial approach adds to the traditional table and graph display formats is that data can be visualized in a more compressed format through lattice (or area) maps. Hence, if needed, all simulation results can be displayed succinctly (as opposed to only subsets of results). Further, area maps visualize spatial patterns of results on the same scale. Thus the results' meaning becomes immediately transparent through the use of proximity and color shading (including in black and white). Finally, the joint display of multiple micro maps makes it possible to efficiently compare simulation results visually across multiple dimensions. Specifically, we propose to visualize the size and power[1] of spatial tests as well as the precision and bias of model estimates by mapping deviations of beta values and standard errors.

The remaining article is structured as follows. In the next section, display formats that are commonly used in spatial econometric simulation experiments are presented. Following is a more detailed introduction of the proposed spatial visualization approach, which includes several examples from spatial simulation experiments. The article closes with a conclusion that discusses limitations of the proposed approach and contextualizes it.

2 Common Displays of Simulation Results

Results from the extensive number of spatial econometric studies that have applied simulation experiments since the 1970s are summarized in Anselin and Rey (1991) and Florax and de Graaff (2004). By contrast, the focus here is on typical display formats from selected examples of this literature. The most common

[1] The size of a test is the probability of rejecting the null hypothesis when it is actually true, whereas the power of a test is the probability of rejecting a false null hypothesis. The null hypothesis of the LM Error, LM Lag and Moran's I is that there is no spatial dependence, i.e., $\rho = 0$ for the lag case and $\lambda = 0$ for the error case (Anselin, 1988).

formats to display simulation results include tables, line graphs (such as QQ plots, discrepancy plots, and size-power curves), and surface response regressions (displayed as tables or graphs). Very recently, studies have begun to use spatial visualizations such as lattice maps, contour line micro plots (2D and 3D), and heat maps. However, these examples differ from the spatial visualization approach proposed in this article in that they often visualize simulated spatial data distributions rather than simulation results related to bias and precision of estimators or size and power of tests. Examples of these more traditional display formats are highlighted next (Table 1 and Figure 1).

Tables remain by far the most commonly used tool to display spatial econometric simulation results. The advantage of tables is that they present numeric results that can be compared at a given precision level, either qualitatively (Anselin and Rey, 1991) or quantitatively through meta-analysis (Florax and de Graaff, 2004). More theoretical spatial econometric articles tend to primarily use tables and statistical summary methods such as response surface analysis to synthesize simulation results (for examples, see Anselin, 1986, Kelejian and Robinson, 1998, Lee, 2004, Kelejian and Prucha, 2007, Baltagi et al, 2007, Lambert et al, 2010, Lee and Liu, 2010). In their basic form, tables are limited to a three-dimensional display of data by categorizing a variable's values by fields and rows. However, in most examples of displaying spatial simulation results, nested tables are used that further subdivide the x- and/or y-axis. A typical example of displaying simulation results for the properties of spatial dependence tests is a rejection frequency table to demonstrate size and power of tests for different spatial parameter values and sample sizes (e.g. Table 1 for the power of statistical tests). Sometimes the results from different tests are nested in the same table. Multiple tables are often used to present additional dimensions, e.g. the results for different data generating processes. Since these tables span multiple pages, it is difficult to efficiently compare results between tables.

Graphs that are commonly used to display spatial simulation results are generally limited to a three-dimensional display of data by plotting a variable's values on an x- and y-axis. While tables display values in discrete row and column categories, one of the strengths of graphs is that they can visualize the distribution of values on continuous x- and/or y-axes. Typical examples of graphical displays in studies that assess the properties of diagnostic tests for spatial dependence include rejection frequency plots, p value plots, p value discrepancy plots and size-power curves (e.g., Anselin and Moreno, 2003 or Baltagi et al, 2003). QQ plots are also used frequently to compare quantiles of hypothesized and observed distributions (e.g., Anselin and Kelejian, 1997 and Lee and Liu, 2010).

Line graphs are most frequently used to compare the performance of spatial estimators, for instance, by plotting the root mean square error against the size of a spatial parameter for different estimators or weights matrices (e.g., Kelejian and Prucha, 1999 or Stakhovych and Bijmolt, 2009). Prominent examples of more statistical summary methods of simulation results include response surface analysis (e.g. Kelejian and Robinson, 1998, Anselin and Moreno, 2003, Egger et al, 2009, Mur and Angulo, 2009) and meta-analysis (Florax and de Graaff,

2004). These results are usually displayed in tabular or line graph format. Although the graphical display of results makes cross-graph comparisons easier than for tables, the constraint to three dimensions within a graph remains.

Some very recent studies are applying maps in the context of simulation studies. However, these visualizations primarily pertain to the generated or estimated distribution of simulated data values for each grid cell on a lattice (where the lattice is the map used to define spatial connectivity in the simulations). For instance, Fingleton and Le Gallo, 2010 (p. 65) use a heat map (or "spatially autocorrelated quadratic surface") to visualize the spatial correlation of their simulated X values on a 15x15 grid. López et al (2010) also visualize the distribution of simulated data values on a grid. Yu et al (2010) (p. 82) apply 10x10 lattice maps to visualize the values of a simulated random field and estimated fields. Going beyond these more standard mapping applications, several other recent spatial simulation studies use visualizations more abstractly to map variations in estimated parameters or probabilities. For instance, López et al (2010)'s 2D and 3D contour maps display the spatial distribution of locally estimated spatial parameters while Mur and Angulo (2009)'s contour maps visualize the probability of correctly selecting different data generating processes.

Our proposed spatial visualization approach combines elements from both these heat map and contour map examples. We use heat maps more abstractly to display and compare simulation results such as estimated parameters, standard errors or rejection rates (as opposed to heat mapping simulated values for a lattice that is part of the simulation design, which is more common). In this sense, the proposed spatial visualization approach supplements common graphical formats like discrepancy plots or size-power curves by, for instance, mapping the bias of spatial estimators or the power of spatial tests. Finally, as different map formats are starting to be used in simulation studies, one of the purposes of this article is to focus attention on the utility of these formats to promote their wider use beyond the still rare examples discussed above. This is a discussion that is absent in these examples.

3 A Spatial Visualization Approach

The contribution of our proposed spatial visualization of simulation results is that it improves the intuitive comparison across simulation dimensions versus the typical table and graph displays discussed above. As Tufte (2001) points out, *our eyes can make a remarkable number of distinctions within a small area* [p. 161]. However, *(. . .) Maps routinely present even finer detail* [p.162]. We take advantage of this and conceptualize the visualization of simulation results abstractly as a spatial map rather than as the more commonly used geospatial (i.e. geographically referenced) map. In this sense, the notion of a spatial map refers to the visual representation of simulation results in terms of location and color. Simulation results are represented through the different intensities of a color's tone, thus turning a table into a choropleth map. Each cell of the table becomes a polygon that is colored following a gradient scheme: the lightest tone

represents the smallest value and the darkest one the largest (this also works in black and white). To ensure comparability, values in the original table need to be reported in the same scale. Then the resulting map makes easy pattern recognition of the spatial distribution of simulation results possible.

In this context, location is not defined geographically but instead reflects an observation that corresponds to two dimensions of the simulation (such as spatial estimators and autoregressive parameters). The color value of a given location adds a third dimension (such as RMSE values). By mapping simulation results in terms of a range of colors and locations, spatial patterns can become visible through the proximity of similar values in nearby locations (this is especially likely when the x- and/or y-axis are ordered as is the case in the two map examples presented below). As in the graphs described above, the starting point for our spatial visualization remains a variable mapped onto an x- and y-axis (three dimensions). Two dimensions are then added by nesting these maps in a 2x2 display that allows for an additional x- and y-axis. For instance, in Fig. 3, β discrepancy values reflecting deviations form the true parameter (Dimension 1) are mapped onto an x-axis of spatial parameter values (Dimension 2) and a y-axis of estimators (Dimension 3). Then these micromaps are replicated for different weights matrices (Dimension 4) as an additional dimension on the y axis and spatial regression model specifications (Dimension 5) as an additional dimension on the x axis. Nesting additional layers onto the x and y axes allows 5 dimensions to be displayed in the nested spatial map format

While this approach is comparable to a nested table, the advantage of the nested map display is that the visual comparison of the simulation results in map format immediately reveals patterns that are not similarly apparent in nested tables or across tables or graphs. Further, these patterns are revealed at different scales: Within a micromap (3 dimensions), within a map (5 dimensions), and across maps with 5 dimensions each, such as for β discrepancies with different weights specifications or for the latter and standard errors. In short, while tables can also nest results, they are unable to efficiently reveal patterns in nested ways, which is made possible by the proposed spatial visualization of simulation results.

The following two subsections illustrate how this technique can add efficient pattern detection to traditionally applied methods. We use two examples: First, a spatial visualization of properties of tests for spatial dependence in linear regression models and second, a map of the precision and bias of non-spatial versus spatial estimators.

3.1 Maps for Test Size and Power

As an illustration of mapping tests properties, we consider the simulation results presented in Anselin and Rey (1991)[2]. The authors compare the properties of Moran's I and Lagrange Multiplier (LM) tests for spatial dependence. They

[2]The results presented here are based on a replication of the experiment undertaken by Anselin and Rey (1991). Due to the randomness of any Monte Carlo experiment, the results may differ.

consider size and power of the tests for both spatial error autocorrelation and spatially lagged dependent variables[3]. Six sample sizes are considered, ranging from 25 to 225 observations. Although they describe results for different spatial weights matrices based on regular lattices, here we present the properties of the tests using only a spatial rook matrix – named $\mathbf{W_1}$ in Anselin and Rey (1991).

Table 1 shows the results of a replication of the simulation in Anselin and Rey (1991) for a sample of 25 observations and considering a nominal Type I error (i.e. significance criterion/nominal size) of 0.05. LM Error and LM Lag indicate the Lagrange Multiplier test for the true spatial process – whether it be error (λ) or lag (ρ). The terms MI Error or MI Lag represent the results of the Moran's I test, also according to the true spatial process.[4]

N	λ or ρ	**LM Error**	**MI Error**	**LM Lag**	**MI Lag**
25	-0.9	0.984	0.98	1	1
	-0.8	0.934	0.924	1	0.995
	-0.7	0.824	0.804	1	0.937
	-0.6	0.684	0.656	1	0.746
	-0.5	0.509	0.479	0.998	0.513
	-0.4	0.343	0.313	0.974	0.33
	-0.3	0.227	0.202	0.871	0.202
	-0.2	0.125	0.114	0.554	0.117
	-0.1	0.067	0.065	0.192	0.065
	0	0.042	0.054	0.055	0.054
	0.1	0.028	0.059	0.133	0.061
	0.2	0.044	0.103	0.442	0.105
	0.3	0.084	0.179	0.781	0.171
	0.4	0.154	0.286	0.953	0.275
	0.5	0.249	0.417	0.995	0.427
	0.6	0.396	0.579	1	0.619
	0.7	0.567	0.727	1	0.82
	0.8	0.724	0.839	1	0.955
	0.9	0.861	0.931	1	0.996

Source: Based on Anselin and Rey (1991)

Table 1: Power of statistical tests over different values for the true spatial parameters (λ,ρ) when significance level is 5%, sample size is 25, and a rook contiguity matrix is used

Another approach is the use of line graphs to represent the properties of the tests. Fig. 1 shows the power of the LM Error test when the nominal size of the test is 5%. These graphs facilitate the comparison between size or power of different test statistics. The case of Fig. 1 emphasizes the distribution of the power of the tests for different sample sizes.[5] The lines represent large amounts of information that are easy to interpret and compare. However, when precision

[3]More information on the tests and the spatial error and lag models can be found in Anselin (1988).

[4]While LM Error and LM Lag are two different tests, the MI Error and MI Lag represent the results of the same Moran's I test for different models. The former is related to a spatial error model, whereas the latter indicates a spatial lag model.

[5] Another graph alternative is the percent plot, or p-p plot where the rejection rate of a test is plotted against its nominal size (Wilk and Gnanadesikan, 1968).

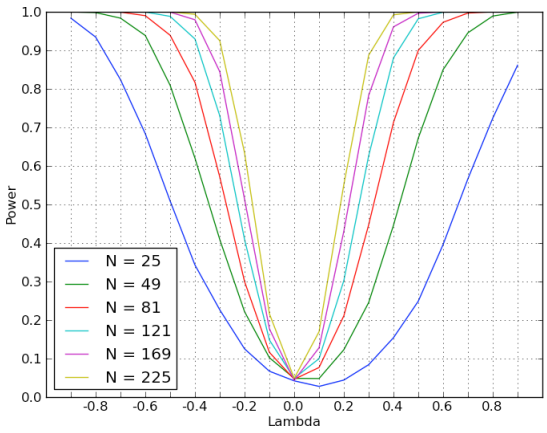

Source: Based on Anselin and Rey (1991).

Figure 1: Power of LM Error test when nominal size is 5%, under different sample sizes and values for the true spatial error parameter (λ), when using a rook contiguity matrix

is needed, such as in the evaluation of the size of tests, graphs such as p-value or discrepancy plots (Davidson and MacKinnon, 1998) are preferred.

One of the limitations of graphs is related to the number of lines shown. Too many lines make it hard to distinguish patterns or colors, and lines crossing each other are difficult to track. Line graphs do facilitate the visualization of results but at the cost of precision and they display little more information than a table.

In comparison, the spatial visualization of test properties can represent information more compactly than tables or graphs, thus facilitating readability and a comparison of results between different tests or sample sizes. Fig. 2 shows the statistical power or 'Rejection Rate' (with increased power indicated by darker shading in the vertical bar to the far right of the graphic) of all the tests considered in this section – LM Error and Moran's I for a spatial error model and LM Lag and Moran's I for a lag model. The figure uses the nested spatial map features to layer on additional information, adding the slider bar to the right and using a second layer of information on the x axis to show the results for all 6 different sample sizes considered in Anselin and Rey (1991).

The nested spatial map in Fig. 2 shows that the power of the tests increases with sample size and with the absolute value of λ or ρ as expected (recall that statistical power increases with greater discrepancy between the true parameter and its hypothesized value). Figure 2 shows that power increases in a more or less symmetric fashion whether the spatial dependence is positive or negative. For the error model, the power curve is steep, indicating that the power of the tests increases rapidly with bigger sample sizes. The figure also shows that Moran's I and LM Error have similar performance in the presence of spatial

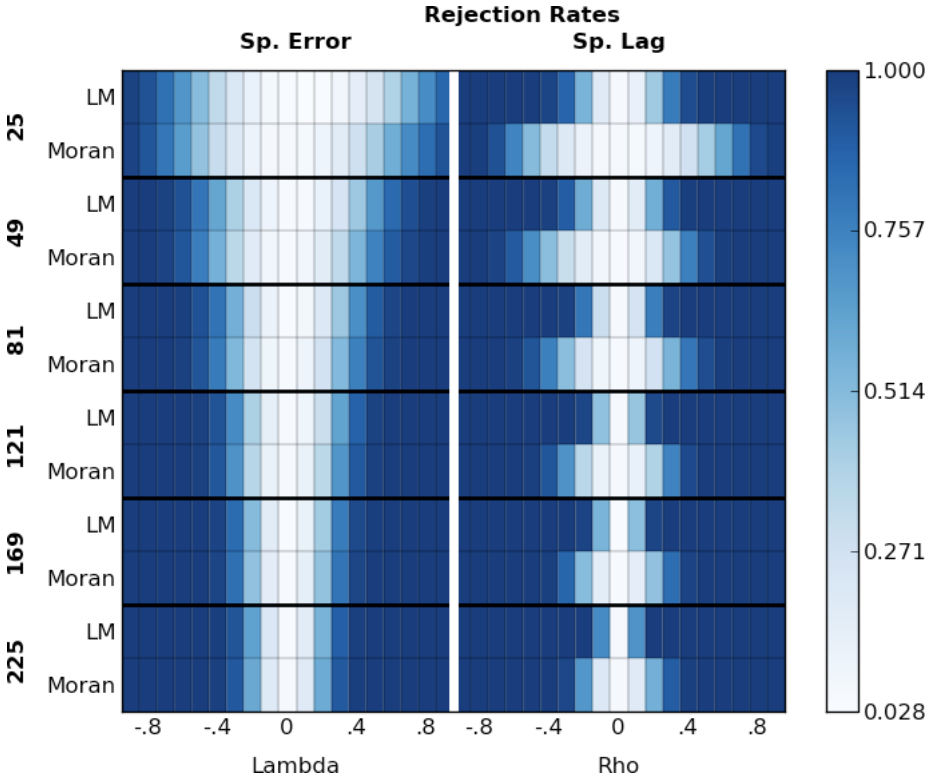

Figure 2: Power of LM Error, LM Lag and Moran's I (Error and Lag model)

dependence in the error. In contrast, the LM lag statistic has clearly superior power in the presence of a spatial lag process. The LM lag achieves a high rejection frequency even for small sample sizes such as N=25 for values of $\rho \geq 0.3$ [6].

If the same amount of information were to be presented in the format of Table 1, six similar tables, or a larger version of the table, would be required: one for each sample size. Or else, if a graph as in Fig. 1 were to be used, four similar graphs would be needed to avoid stacking lines on the same graph.

3.2 Maps for Model Bias and Precision

The next example is based on research by Anselin and Arribas-Bel (2011), which assesses the claim that spatial fixed effects can account for spatial autocorrelation. As an empirical illustration, the authors provide evidence from several Monte Carlo experiments; they simulate different scenarios 10,000 times each and average the values of the coefficient estimates ("Betas") and their standard errors ("SEs") across simulations to study the influence of several types of spatial data generating processes on different estimation methods. In particular, they consider the following specifications for two different datasets: two spatial configurations (assumed queen or block-wise dependence); and two processes, spatial error or spatial lag, operating at eight different degrees of spatial autocorrelation (λ and ρ respectively). For each of them, they estimate three models, namely OLS, OLS with fixed effects ("FE") and a spatial model ("KP" for Kelejian and Prucha (1998)). This setup results in 192 (2 x 2 x 2 x 8 x 3 = 192) combinations. Since the focus is on looking at the estimation bias in the betas and precision induced by the spatial autocorrelation in the data, they report the average value for each case.

Fig. 3 shows three possible options to present the results. The first one (a) depicts the traditional table for the spatial error case. The second one (b) displays the density distribution of the coefficient estimate values (horizontal axis) for OLS with fixed effects by the extent of spatial autocorrelation for the queen contiguity case. In this case, larger deviation from the true value (1,0) implies larger bias, as ρ increases. The maps in Fig. 3 (c) show the results for the parameter estimates (average deviation from the true value) and the standard errors (SEs) for the two spatial weights, the three estimation methods (OLS, FE and KP) and the eight values of spatial autocorrelation. Each lattice covers one type of value (beta estimates on the left and SEs on the right). For each map, the horizontal axis represents different sizes of spatial autocorrelation for the spatial error (λ) or spatial lag (ρ) generating processes. The vertical axis shows each of the methods for the two assumed spatial dependence processes. An additional nested dimension across the horizontal axis allows the display of both types of spatial models ("Sp. Error" or "Sp Lag"). And an additional dimension on the side of the graphic makes the display of two types of spatial

[6] For more information on the results and comparison between LM Error and LM Lag, please see Anselin and Rey (1990).

		Rho Values							
		0.0	0.01	0.1	0.25	0.5	0.75	0.9	0.99
OLS	Beta	1.0	1.0	1.002	1.013	1.059	1.182	1.388	2.01
	SE	0.013	0.013	0.013	0.014	0.015	0.021	0.035	0.123
	MSE	0.0	0.0	0.0	0.0	0.004	0.033	0.151	1.025
FE	Beta	1.0	1.0	1.001	1.01	1.051	1.16	1.328	1.689
	SE	0.013	0.013	0.013	0.014	0.015	0.02	0.031	0.077
	MSE	0.0	0.0	0.0	0.0	0.003	0.026	0.108	0.477
KP	Beta	1.0	1.0	1.0	1.0	1.0	1.0	1.0	1.0
	SE	0.013	0.013	0.013	0.013	0.013	0.014	0.014	0.014
	MSE	0.0	0.0	0.0	0.0	0.0	0.0	0.0	0.0

(a) Table

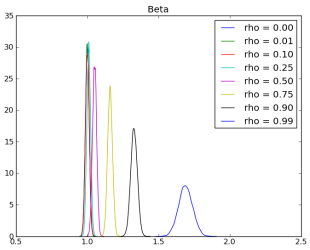

(b) Distribution density

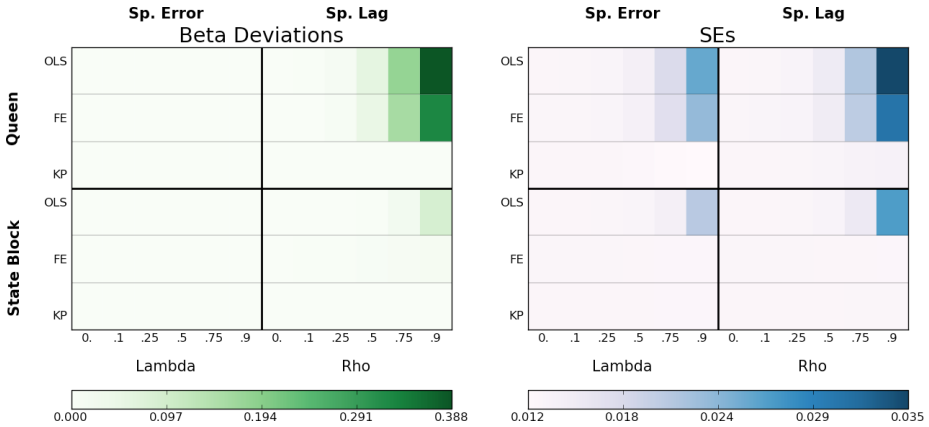

(c) Simulation map

Figure 3: Comparisons of table, line graph and nested spatial map display of simulation results

dependence processes possible ("State Block", "Queen"). Finally, the bar at the bottom of the graphic displays the degree of deviation of beta from the true value (left) as well as the standard error (right).

Among the three, the map allows for a quick visualization and presents in a clear way the main "message" of the data. It is also the device that condenses the largest amount of information: note that, in order to represent the information in Fig. 3 (c), it would take four tables like the one in (a) or twelve plots as in (b).

4 Conclusion

We propose spatial visualization of simulation results as a useful supplement to tables and graphs rather than as alternative substitute for them. Each device has its benefits and disadvantages. Tables excel at accuracy, but do poorly at showing the main message in a succinct way. Density graphs intuitively inform

about the estimates beyond the mean but do not condense information very well as the space needed increases rapidly with the number of dimensions to portray. Maps condense much in little space, visually communicating statistical information and displaying the main picture at once; however, they are not optimal for displaying particular values or distribution of values. Because simulation modeling approaches to assess statistical properties of estimators inherently contain many dimensions, enhanced visualization methods are particularly useful. We showed using a nested spatial map (Figure 1) the superior power inherent in spatial lag models, as compared to spatial error models, all else the same –which is a powerful visual reminder of this important statistical property which would otherwise remain obscure. The nested spatial maps presented in this article are only two examples of how one might spatially visualize simulation results. Many other extensions are possible, e.g. mapping root mean squared errors (RMSEs) instead of beta deviations or combining other simulation dimensions in the visualization. This work complements efforts begun by Tufte (2001) and others, to use powerful visualization techniques to enhance translation of complex information.

Acknowledgements The authors would like to thank Luc Anselin and Lee Mobley for valuable feedback. The research in this paper was supported in part by National Cancer Institute Grant 1R01CA126858-01A1. The content is solely the responsibility of the authors and does not necessarily represent the official views of the National Cancer Institute, or the National Institutes of Health.

References

Anselin L (1986) Non-nested tests on the weight structure in spatial autoregressive models: Some Monte Carlo results. Journal of Regional Science 26(2):267–284

Anselin L (1988) Spatial econometrics. Kluwer Academic Publishers Dordrecht

Anselin L, Arribas-Bel D (2011) Spatial Fixed Effects and Spatial Dependence, Working Paper, GeoDa Center for Geospatial Analysis and Computation.

Anselin L, Kelejian H (1997) Testing for spatial error autocorrelation in the presence of endogenous regressors. International Regional Science Review 20(1):153

Anselin L, Moreno R (2003) Properties of tests for spatial error components. Regional Science and Urban Economics 33(5):595 – 618

Anselin L, Rey S (1990) The performance of tests for spatial dependence in a linear regression. Technical Report, National Center for Geographic Information and Analysis (NCGIA), University of California, Santa Barbara

Anselin L, Rey S (1991) Properties of tests for spatial dependence in linear regression models. Geographical Analysis 23(2):112–131

Baltagi BH, Song SH, Koh W (2003) Testing panel data regression models with spatial error correlation. Journal of Econometrics 117(1):123 – 150

Baltagi BH, Egger P, Pfaffermayr M (2007) A Monte Carlo study for pure and pretest estimators of a panel data model with spatially autocorrelated disturbances. Annals of Economics and Statistics 87/88(3):11–38

Davidson R, MacKinnon JG (1998) Graphical methods for investigating the size and power of hypothesis tests. The Manchester School 66(1):1–26

Egger P, Larch M, Pfaffermayr M, Walde J (2009) Small sample properties of maximum likelihood versus generalized method of moments based tests for spatially autocorrelated errors. Regional Science and Urban Economics 39(6):670 – 678

Fingleton B, Le Gallo J (2010) Endogeneity in a spatial context: Properties of estimators. In: Páez A, Buliung RN, Gallo JL, Dallerba S (eds) Progress in Spatial Analysis, Advances in Spatial Science, Springer Berlin, pp 59–73

Florax R, de Graaff T (2004) The performance of diagnostic tests for spatial dependence in linear regression models: a meta-analysis of simulation studies. In: Anselin L, Florax R, Rey S (eds) Advances in spatial econometrics: methodology, tools and applications, Springer Berlin Heidelberg, pp 29–65

Kelejian H, Prucha I (1998) A generalized spatial two-stage least squares procedure for estimating a spatial autoregressive model with autoregressive disturbances. The Journal of Real Estate Finance and Economics 17(1):99–121

Kelejian H, Prucha I (1999) A Generalized Moments Estimator for the Autoregressive Parameter in a Spatial Model. International Economic Review 40(2):509–533

Kelejian H, Prucha I (2007) HAC estimation in a spatial framework. Journal of Econometrics 140(1):131–154

Kelejian HH, Robinson DP (1998) A suggested test for spatial autocorrelation and/or heteroskedasticity and corresponding Mnote Carlo results. Regional Science and Urban Economics 28(4):389 – 417

Lambert DM, Brown JP, Florax RJ (2010) A two-step estimator for a spatial lag model of counts: Theory, small sample performance and an application. Regional Science and Urban Economics 40(4):241 – 252

Lee LF (2004) Asymptotic distributions of quasi-maximum likelihood estimators for spatial autoregressive models. Econometrica 72(6):1899–1925

Lee LF, Liu X (2010) Efficient gmm estimation of high order spatial autoregressive models with autoregressive disturbances. Econometric Theory 26(01):187–230

López F, Mur J, Angulo A (2010) Local estimation of spatial autocorrelation processes. In: Páez A, Buliung RN, Gallo JL, Dallerba S (eds) Progress in Spatial Analysis, Advances in Spatial Science, Springer Berlin Heidelberg, pp 93–116

Mur J, Angulo A (2009) Model selection strategies in a spatial setting: Some additional results. Regional Science and Urban Economics 39(2):200 – 213

Stakhovych S, Bijmolt TH (2009) Specification of spatial models: A simulation study on weights matrices. Papers in Regional Science 88(2):389–408

Tufte ER (2001) The Visual Display of Quantitative Information, 2nd edn. Graphics Press

Wilk MB, Gnanadesikan R (1968) Probability plotting methods for the analysis of data. Biometrika 33(1):1 – 17

Yu HL, Christakos G, Bogaert P (2010) Dealing with spatiotemporal heterogeneity: The generalized bme model. In: Páez A, Buliung RN, Gallo JL, Dallerba S (eds) Progress in Spatial Analysis, Advances in Spatial Science, Springer Berlin Heidelberg, pp 75–92